THE JOURNAL OF PHYSICAL CHEMISTRY B

Article

pubs.acs.org/JPCB

Picosecond Solvation and Rotational Dynamics: An Attempt to Reinvestigate the Mystery of Alcohol–Water Binary Mixtures

Debasis Banik, Arpita Roy, Niloy Kundu, and Nilmoni Sarkar*

Department of Chemistry, Indian Institute of Technology, Kharagpur 721302, West Bengal, India

Supporting Information

ABSTRACT: In this article, we have investigated the anomalous behavior of two alcohol–water (*tert*-butyl alcohol (TBA)–water and ethanol–water) binary mixtures using femtosecond fluorescence upconversion technique. Recently, Gupta and Patey (Gupta, R.; Patey, G. N. *J. Chem. Phys.* **2012**, 137, 034509(1)–034509(12)) have used four force fields to simulate TBA–water binary mixtures. Surprisingly, two of them do not identify any aggregation of TBA molecules. We have calculated average solvation time of Coumarin 480 (C480) using two different methods. Our results indicate slowdown in solvation time in the mole fraction ranges X_T = 0.09–0.15, X_T = 0.40–0.46 and X_E = 0.06–0.08, X_E = 0.20–0.25 for TBA–water and ethanol–water binary mixtures, respectively. Additionally, we have detected another anomalous region at $X_T \sim 0.03$. Slow solvation responses in the ranges X_T = 0.40–0.46 and X_E = 0.20–0.25 are probably due to the higher shear viscosity of the medium. However, X_T = 0.09–0.15 and X_E = 0.06–0.08 are the manifestation of aggregation induced structural transition of alcohol molecules. Hindered rotation of C480 in the ranges X_T = 0.04–0.09 and X_E = 0.03–0.07 corroborates our solvation dynamics results. From temperature dependent anisotropy measurements, we have shown that aggregation of alcohol molecules increases with increase in temperature.

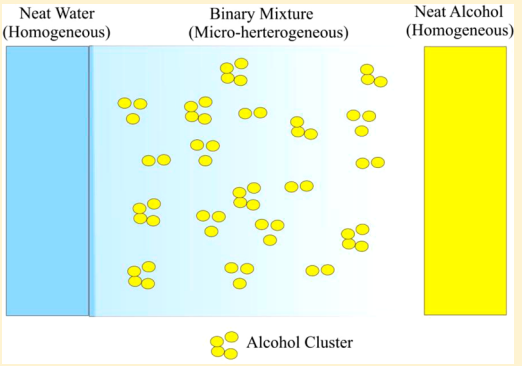

1. INTRODUCTION

Anomalous phenomena are ubiquitous and fundamentally important especially in chemistry. For example, water exhibits anomalous expansion of volume on cooling below 4 °C which is directly related to its structural aspects.[1] Therefore, in recent years, much more effort has been devoted to elucidate the microscopic origin of different anomalous systems like binary mixtures. Binary mixtures have aroused considerable attention in the scientific communities due to their nonideal thermodynamic and transport properties, such as viscosity,[2−4] density,[3] mean molar volume,[5,6] diffusion coefficient,[7−9] excess entropy,[10,11] heat of formation,[10] surface tension,[12,13] adiabatic and isothermal compressibility,[14−16] sound attenuation coefficient,[17−19] excess heat capacity,[20] etc. Experimental and simulation studies have indicated the microheterogeneity as a probable reason for this nonideal behavior exhibited by binary mixtures.

Usually, small amphiphilic molecules such as dimethyl sulfoxide (DMSO),[21−26] dioxane,[27] ethanol,[28,29] 1-propanol,[30] *tert*-butyl alcohol (TBA),[31] which contain both hydrophilic and lipophilic moieties, have a tendency to form microheterogeneous aggregates upon mixing with water. A delicate hydrophilic–lipophilic balance ("Janus effect") maintains the microheterogeneity within the solution, although the solution remains homogeneous in the macroscopic length scale.[32] The most common feature that has been observed in almost all the aqueous–amphiphilic binary mixtures is the appearance of low concentration anomalies. For example, several thermodynamic properties of aqueous (solvent) DMSO, ethanol, and TBA (solute) exhibit deviation at very low solute mole fractions of 0.15, 0.10, and 0.04, respectively.[5,6] Furthermore, various applications as a "designer solvent" (desired properties can be obtained only by changing the composition) in organic chromatography as well as in reaction media make these systems curious and interesting ones.[33,34]

With the advent of the "iceberg" model by Frank and Evans at the middle of twentieth century, there have been many attempts to correlate this idea with the anomalous behavior of aqueous–amphiphilic binary mixtures.[35] However, this model was not supported by modern diffraction studies.[36−39] In another model, it was proposed that TBA molecules form clathrate–hydrate with water.[40] Euliss et al. mentioned that the globular shape of *tert*-butyl group perfectly matches with the spherical cavity of clathrate formed by water molecules, thereby forming fully miscible aqueous solution at any proportion.[41] They have proposed two types of aggregates, i.e., TBA–water and water–water aggregates in the form of clathrate-type structure. Fujiyama et al. studied the TBA–water binary mixture by Rayleigh light scattering experiments and interpreted their results in terms of stoichiometrically formed clathrates between TBA and water.[42] Sengers et al. speculated that long-lived metastable clathrate-like precursors are respon-

Received: May 23, 2015
Revised: June 28, 2015

DOI: 10.1021/acs.jpcb.5b04931
J. Phys. Chem. B XXXX, XXX, XXX–XXX

sible for the microscopic concentration fluctuations and mesoscopic inhomogeneities in aqueous TBA solution.[43] However, neutron diffraction studies using H/D isotopic substitution predicted that the association of TBA molecules in TBA−water binary mixture is mainly governed by the interaction of nonpolar tertiary butyl groups.[44,45] In another study, Soper et al. found that the local structure of water in concentrated methanol−water solution was close to neat water.[36] This observation discarded the possibility of clathrate formation. They have explained the negative excess entropy observed in this system in terms of incomplete mixing of two components at the molecular level. The aggregation of TBA molecules was further supported by the small angle neutron scattering experiments.[38,46]

Computer simulation has a significant contribution in determining structural and dynamical characteristics of the binary mixtures. Bagchi and co-workers have detected two anomalous regions of DMSO−water binary mixtures through molecular dynamics simulation.[21−24] Earlier simulation studies have proved the existence of 1DMSO:2H_2O in equilibrium with 2DMSO:1H_2O complex in aqueous DMSO solution.[26,47] Tanaka et al. performed molecular dynamics simulation in aqueous−TBA solution. Their study indicates that the aggregation of TBA molecules from very dilute to 8 mol % of TBA concentration was governed by the hydrophobic contact of *tert*-butyl groups, whereas, with increasing TBA concentration (at 17 mol % of TBA), the association occurs through hydrogen bonding interactions between TBA molecules.[48] Kusalik et al. simulated two dilute solutions (2 mol % and 8 mol % of TBA) of the same binary mixture and noted spontaneous aggregation of TBA at 8 mol %.[49] Lee et al. have used a new force field for atomistic simulations of TBA−water binary mixture and noticed trimeric TBA aggregates in dilute aqueous solution of TBA (X_T = 0.06).[50] On the basis of Kirkwood−Buff theory, Shulgin et al. predicted two types of clusters (alcohol-rich and water-rich clusters) present in this system.[51] Very recently, Banerjee et al. observed percolation transition of TBA and water molecules at 0.05 and 0.45 mole fraction of TBA, respectively, whereas in the case of ethanol−water binary mixture it appears in the range of 0.06−0.10 mole fraction of ethanol.[52,53] By quantifying the lifetime, the same group has proposed the stability order (ethanol−water < DMSO−water < TBA−water) of these microheterogeneous aggregates.[54]Gupta and Patey have performed molecular dynamics simulation in TBA−water binary mixture using four different force fields. Surprisingly, two of them are able to detect the aggregation of TBA molecules, whereas the remaining two do not indicate any aggregation. The overall conclusion of their study indicates that the hydrophobic interactions between *tert*-butyl groups are responsible for self-aggregation of TBA molecules.[55] Very recently, Ben-Amotz[56] and Rankin[57] have shown that there are no more hydrophobic contacts in aqueous solutions of alcohols ranging from methanol to TBA than in random mixtures of the same concentration. Therefore, hydrophobic interactions between small hydrophobic groups are weaker than thermal energy fluctuations. Finney and co-workers observed maximum clustering of TBA at 80 °C through isotope substitution neutron scattering experiment. Aggregation tendency decreases with further increase in temperature.[58] Recently, Anisimov et al. have observed stable mesoscale inhomogeneities in TBA−water binary mixture only in the presence of a more hydrophobic third component (cyclohexane). They concluded that these droplets could be extremely long-lived, being stable for over a year.[59]

Although a lot of molecular dynamics simulations have been performed on these (binary mixture) systems, experimental support in favor of these anomalous behaviors are not extensive.[28−31,60,61] Solvation dynamics is an important spectroscopic tool to investigate the dynamical relaxation of solvent molecules around an excited state dipole. This method has been extensively used to investigate the dynamical properties in solutions and organized assemblies.[62−83] However, there are very few reports of solvation dynamics in binary mixtures.[30,84−86] Shirota et al. showed the anomalous behavior of 1-propanol−water system in the range X_{ProH} = 0.15−0.25 by monitoring solvation response around Coumarin 153 (C153) molecule.[30] Ghosh et al. used three coumarin dyes [C153, Coumarin 480 (C480), and Coumarin 343 (C343)] as solvation probe to detect multiple anomalous regions in dimethyl sulfoxide (DMSO)−glycerol (GLY) binary mixtures.[60] Very recently, we have detected two anomalous regions of DMSO−water binary mixtures at X_D = 0.12−0.17 and X_D = 0.27−0.35 using C480 as a solvation probe.[61]

There has been an increasing interest in studying rotational dynamics of different probe molecules in aqueous binary mixtures and room temperature ionic liquids.[87−91] Dutt et al.[87] investigated rotational motions of four dye molecules in aqueous TBA binary mixture. They suggested that simple hydrodynamic theory due to Stokes−Einstein−Debye (SED) is not adequate to describe the entire region of the plot of τ_r vs η. SED theory is only applicable for a water rich region (low viscosity region). However, in the case of an alcohol rich region dielectric friction theory has to be considered to mimic the bivalued profile of τ_r vs η. Krishnamurthy et al. found a hook-type profile in the τ_r vs η plot in the case of three kinds of dyes in hexamethylphosphoramide (HMPA)−water binary mixtures. They also concluded that dielectric friction provides a satisfactory description of rotational dynamics.[88]

In this present article, we have investigated composition dependent anomalous behavior of TBA−water and ethanol−water binary mixtures by monitoring ultrafast solvation response around a solvation probe Coumarin 480 (C480) (Scheme 1) using a femtosecond fluorescence upconversion technique. Our results indicate slowdown in solvation time in the ranges X_T = 0.09−0.15, X_T = 0.40−0.46 and X_E = 0.06−0.08, X_E = 0.20−0.25 for TBA−water and ethanol−water binary mixtures, respectively. Additionally, we have detected another anomalous region at $X_T \sim 0.03$ in TBA−water binary mixture. Note that most of the thermodynamic properties exhibit deviation from ideal behavior around this region. We have also

Scheme 1

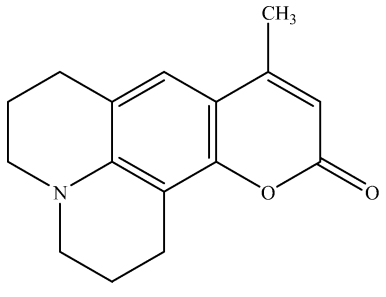

Coumarin 480

DOI: 10.1021/acs.jpcb.5b04931
J. Phys. Chem. B XXXX, XXX, XXX−XXX

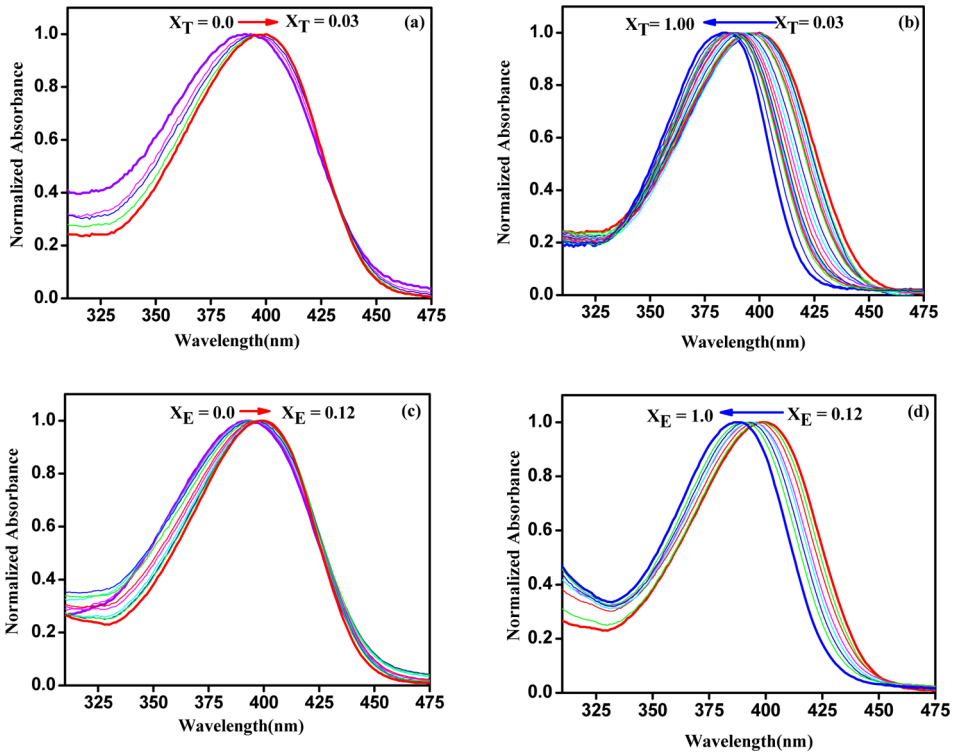

Figure 1. Steady-state UV−vis absorption spectra (normalized) of C480 in TBA−water [(a) X_T = 0.0−0.03, (b) X_T = 0.03−1.00] and ethanol−water [(c) X_E = 0.0−0.12, (d) X_E = 0.12−1.00] binary mixture.

measured rotational reorientation times of C480 in these two binary mixtures. The hindered rotation of C480 in the ranges X_T = 0.04−0.09 and X_E = 0.03−0.07 corroborates our solvation dynamics result. To the best of our knowledge, this is the first work of ultrafast solvation dynamics in TBA−water and ethanol−water binary mixtures.

2. EXPERIMENTAL SECTION

2.1. Materials. Laser grade Coumarin 480 (C480) was purchased from Exciton and used as received without further purification. We followed the procedure described in ref 92 for distillation of ethanol. Spectroscopic grade *tert*-butyl alcohol (TBA) from Spectrochem Pvt. Ltd., India, distilled ethanol, and triple distilled Milli-Q water were used to prepare all the solutions of TBA−water and ethanol−water binary mixtures for experimental purposes.

2.2. Sample Preparation. We prepared three individual stock solutions of C480 in water, TBA, and ethanol in three separate volumetric flasks. After keeping them for 24 h at room temperature we measured the absorption spectra of three individual stock solutions. Then, we adjusted the absorbance (at absorption maxima) values of three neat solutions near about 0.30. All the experiments were carried out with these three adjusted stock solutions.

2.3. Instruments and Methods. Steady-state UV−vis absorption and fluorescence spectra were collected using a Shimadzu (model UV 2450) UV−vis spectrophotometer and a Hitachi (model no. F-7000) spectrofluorimeter, respectively. For steady-state measurements, all the samples were excited at 408 nm and emissions were collected from 420 to 650 nm.

Time-resolved anisotropy decays were recorded using a time-correlated single photon counting (TCSPC) picosecond setup. The detailed experimental setup of this TCSPC instrument is described in our previous publication.[93] In brief, all the samples were excited using a picosecond diode laser at 408 nm (IBH, UK, Nanoled) and the signals were collected using a Hamamatsu microchannel plate photomultiplier tube (3809U). For the anisotropy decays, we used a motorized polarizer on the emission side to collect the emission intensities at parallel ($I_\parallel$) and perpendicular ($I_\perp$) polarizations until a certain count difference between parallel ($I_\parallel$) and perpendicular ($I_\perp$) decay was reached, and the anisotropy decay function $r(t)$ was constructed from these $I_\parallel$ and $I_\perp$ decays using the equation

$$r(t) = \frac{I_\parallel(t) - GI_\perp(t)}{I_\parallel(t) + 2GI_\perp(t)} \quad (1)$$

where G is the instrument correction factor for detector sensitivity to the polarization of the emission. For our experimental setup, the value of the G factor at the detection wavelength was 0.6. The instrument response function for our setup is ∼100 ps. Time-resolved anisotropy decays were analyzed using IBH DAS-6 decay analysis software.

Femtosecond fluorescence traces were collected using a fluorescence upconversion instrument (FOG 100, CDP, Russia). The details of this experimental setup have been given in an earlier publication.[94] Briefly, all the samples were excited using a second harmonic (400 nm) of a mode-locked Ti-sapphire laser (Tsunami, Spectra-Physics). A nonlinear crystal (1 mm BBO, θ = 25°, ϕ = 90°) was used for frequency doubling of the fundamental beam (800 nm) to generate the expected excitation source. Here it is notable that the fluorescence emitted from the sample was not measured directly but it was upconverted in a nonlinear crystal (0.5 mm BBO, θ = 38°, ϕ = 90°) using the fundamental beam as a gate pulse. The upconverted light was then dispersed in a monochromator and detected using photon counting electronics. The cross-correlation measured between the second

DOI: 10.1021/acs.jpcb.5b04931
J. Phys. Chem. B XXXX, XXX, XXX−XXX

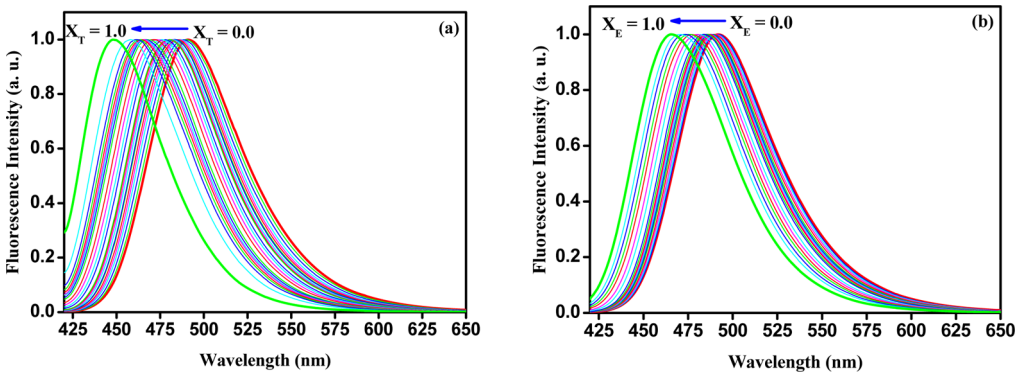

Figure 2. Steady-state emission (normalized) spectra of C480 in TBA−water [(a) X_T = 0.0−1.00] and ethanol−water [(b) X_E = 0.0−1.00] binary mixture.

harmonic and the fundamental had a full-width at half-maximum (fwhm) of 300 fs (fs).

2.4. Viscosity Measurements. Viscosities of TBA−water and ethanol−water binary mixtures were measured using a Brookfield DV-II+ Pro viscometer at 298 K. We also measured the temperature dependent viscosities of two binary mixture (X_T = 0.09 and X_E = 0.06) ranging from 278 to 302 K at a regular interval of 4 °C. The temperature was maintained constant by circulating water through the sample holder using a JEIOTECH circulating bath (RW-0525GS). The error limit of the instrument in the measurement of temperature is ±0.1 °C.

3. RESULTS AND DISCUSSION

3.1. Steady-State Absorption and Emission Studies. Figure 1 shows the steady-state UV−vis absorption spectra of C480 in TBA−water (Figure 1a,b) and ethanol−water (Figure 1c,d) binary mixture covering the whole region. Absorption maxima of C480 in water, ethanol, and TBA are centered at 391, 387, and 384 nm, respectively. In both binary mixtures, absorption shift of C480 can be described through two stages. Initially, with the addition of TBA/ethanol to water, absorption maxima of C480 exhibit a red shift up to the mole fraction X_T = 0.03 and X_E = 0.12, respectively (Figure S1a,b, Supporting Information). The amount of bathochromic shift is almost the same (∼510 cm^{-1}) in two binary mixtures. After that, further addition of TBA/ethanol shifts the absorption maxima toward the blue end. On the other hand, emission maxima of C480 in water, ethanol, and TBA are 491, 465, and 447 nm, respectively. In contrary to the absorption maxima, emission maxima of C480 exhibit a regular blue shift from initial addition of TBA/ethanol to water (Figure 2a,b and Figure S1c,d, Supporting Information). The hypsochromic shifts in TBA−water and ethanol−water binary mixtures are ∼2000 and ∼1150 cm^{-1}, respectively. Steady-state Stokes shift decreases with increasing alcohol content in both binary mixtures (Figure S1e,f, Supporting Information). Interestingly, the decrease is more prominent up to the mole fraction X_T = 0.03 and X_E = 0.12.

Recently, we have studied solvation dynamics of C480 in DMSO−water binary mixtures.[61] Interestingly, in this work we have found a similar trend in the absorption (red shift followed by blue shift) and emission (blue shift) shifts of C480 in TBA−water and ethanol−water binary mixtures as we observed earlier in the case of DMSO−water binary mixtures. We have qualitatively explained the unusual absorption and emission shifts of C480 using a model discussed by Hynes et al. in our previous publication.[61,95] In brief, the absorption transition energy (E_{abs}) and emission transition energy (E_{em}) can be obtained from the equations

$$E_{abs} = V_{eq}^{adia} + \Lambda_s^{ex} \qquad E_{em} = V_{eq}^{adia} - \Lambda_s^{g} \tag{2}$$

where V_{eq}^{adia} is the equilibrated energy gap between adiabatic ground and excited states. Λ_s^g and Λ_s^{ex} are the adiabatic solvent reorganization energies in ground and excited states, respectively. Before X_T = 0.03 and X_E = 0.12, Λ_s^g and Λ_s^{ex} have significant contributions on E_{em} and E_{abs}, respectively. As a result, the factor (V_{eq}^{adia} + Λ_s^{ex}) decreases and (V_{eq}^{adia} − Λ_s^{g}) increases on going from X_T = 0.0 to 0.03 and X_E = 0.0 to 0.12. This is the probable reason for the initial red shift of absorption spectra. After these regions (X_T = 0.03, X_E = 0.12), E_{abs} and E_{em} completely depend on the factor V_{eq}^{adia}. As the factor V_{eq}^{adia} increases with increasing alcohol content, we have observed a pronounced blue shift after X_T = 0.03 and X_E = 0.12 (detailed discussion has been given in the Subsection III B of ref 61). Note that we reported similar behavior of dioxane−water mixture using a hemicyanine dye (LDS-698).[27]

3.2. Unusual Solvation Trends in TBA−Water and Ethanol−Water Binary Mixtures. In a recent molecular dynamics simulation study, Patey and co-workers have pointed out that the aggregation tendency of alcohol molecules is entirely dependent on employed force fields.[55] They have also pointed out that all four force fields in their 64000 particle simulations are not able to represent the real system as they have observed demixing-like behavior for $X_T \geq 0.1$ in TBA−water binary mixture. However, in reality TBA−water binary mixture is miscible in all proportions. Therefore, by considering these aspects it is quite interesting to investigate this system from the experimental point of view. Recently, we have detected two anomalous regions of DMSO−water binary mixtures (X_D = 0.12−0.17 and X_D = 0.28−0.35) by collecting ultrafast solvation response of C480.[61] In that study, we have used two well-known methods of solvation dynamics, i.e., "spectral-reconstruction method" and "single-wavelength measurement method" to detect the unusual solvation trends in the above binary mixture. In a continuation of our previous study, in this work we have chosen two alcohol−water (the two alcohols are widely different with respect to their hydrophobic residue) binary mixtures to make a comparison between their anomalous behavior through solvation dynamics. At first, we have collected upconversion traces of C480 at different wavelengths covering the entire region of emission spectra of TBA−water and ethanol−water binary mixture. To fit the upconversion traces, we have measured long decay components

DOI: 10.1021/acs.jpcb.5b04931
J. Phys. Chem. B XXXX, XXX, XXX−XXX

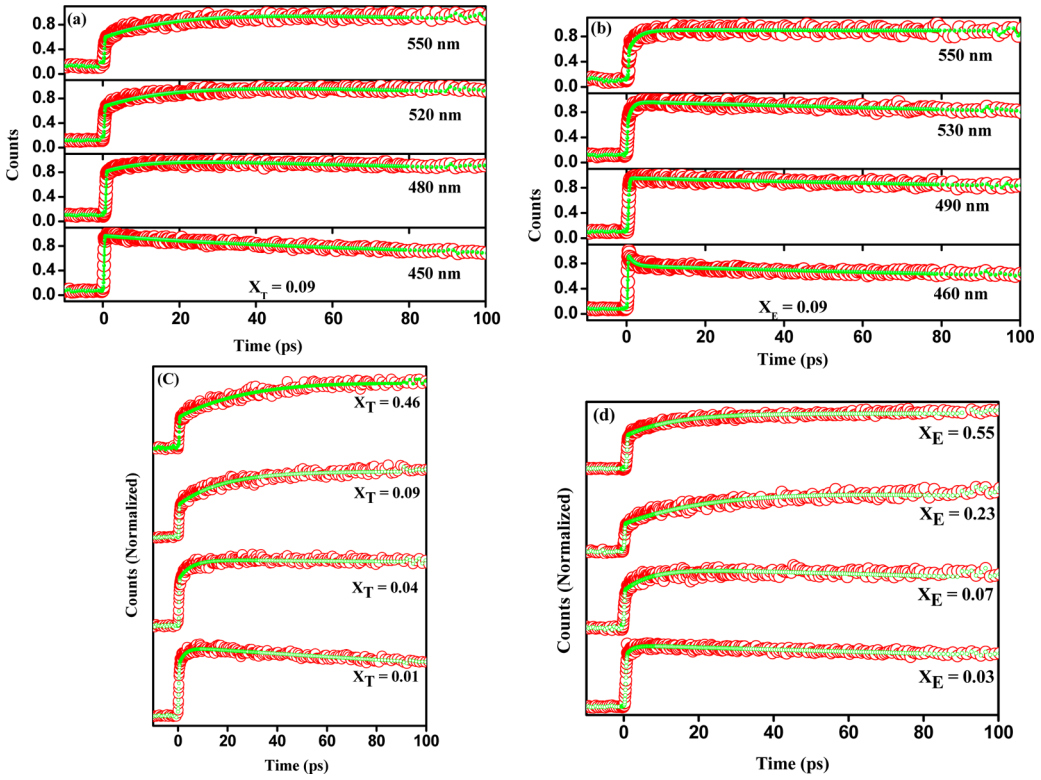

Figure 3. Fluorescence upconversion traces (normalized) of C480 in TBA–water [(a) X_T = 0.09 and (c) at 550 nm with increasing mole fraction of TBA] and ethanol–water [(b) X_E = 0.09 and (d) at 550 nm with increasing mole fraction of ethanol] binary mixtures.

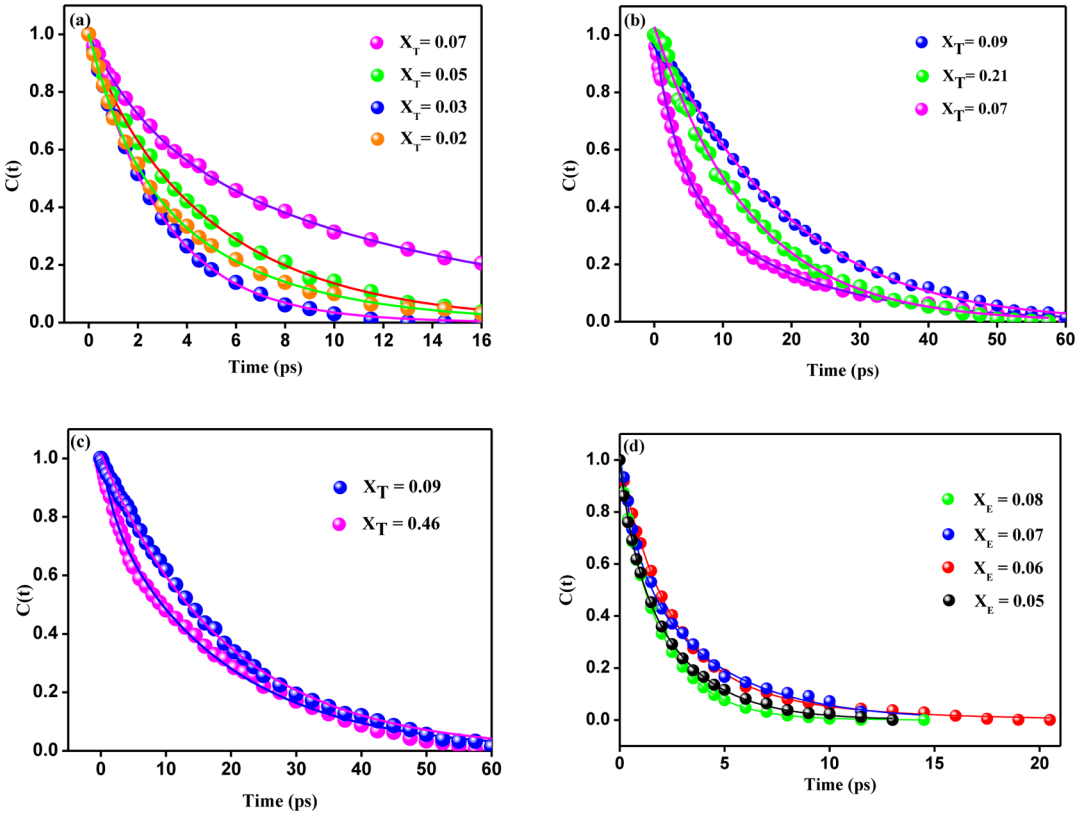

Figure 4. Decay plots of solvent correlation function $C(t)$ of C480 in TBA–water [(a) X_T = 0.02, 0.03, 0.05, 0.07; (b) X_T = 0.07, 0.09, 0.21; (c) X_T = 0.09, 0.46] and ethanol–water [(d) X_E = 0.05, 0.06, 0.07, 0.08] binary mixtures.

of C480 in these two binary mixtures using our TCSPC setup. During fitting, these long decay components were kept constant to evaluate the ultrashort components. Upconversion traces of C480 at different mole fractions of TBA and ethanol

DOI: 10.1021/acs.jpcb.5b04931
J. Phys. Chem. B XXXX, XXX, XXX–XXX

in TBA−water and ethanol−water binary mixtures are shown in Figure 3a−d.

Solvation dynamics is defined by a solvent correlation function $C(t)$ which is denoted as

$$C(t) = \frac{\nu(t) - \nu(\infty)}{\nu(0) - \nu(\infty)} \tag{3}$$

where $\nu(0)$, $\nu(t)$, and $\nu(\infty)$ are the peak frequencies at time zero, intermediate time, and infinity, respectively. The decays of $C(t)$ are fitted by a single or biexponential function depending on its nature. The expression for a biexponential $C(t)$ is given in eq 4,

$$C(t) = a_1 \exp^{-t/\tau_1} + a_2 \exp^{-t/\tau_2} \tag{4}$$

where τ_1 and τ_2 are the solvation times with amplitudes of a_1 and a_2, respectively. The $C(t)$ versus time (t) plots of C480 in TBA−water and ethanol−water binary mixtures are shown in Figure 4a−d. Then the average solvation time $\langle\tau_s\rangle$ is calculated using the following equation:

$$\langle\tau_s\rangle = a_1\tau_1 + a_2\tau_2 \tag{5}$$

Time-resolved emission spectra (TRES) were constructed following the procedure of Fleming and Maroncelli.[67] The TRES at a given time t, $S(\lambda;t)$, is obtained by the fitted decays, $D(\lambda;t)$, by relative normalization to the steady-state spectrum $S_0(\lambda)$, as follows:

$$S(\lambda;\, t) = D(\lambda;\, t)\frac{S_0(\lambda)}{\int_0^\infty D(\lambda;\, t)\, \mathrm{d}t} \tag{6}$$

Each (TRES) was fitted by a "log-normal line shape function", which is defined as

$$g(\nu) = g_0 \exp\left[(-\ln 2)\left(\frac{\ln[1 + 2b(\nu - \nu_p)/\Delta]}{b}\right)^2\right] \tag{7}$$

where g_0, b, ν_p, and Δ are the peak height, asymmetric parameter, peak frequency, and width parameter, respectively. The TRES plots of C480 at $X_T = 0.09$ and $X_E = 0.06$ are shown in Figures S2a and S2b of the Supporting Information. Solvation time calculated through this procedure is called "spectral re-construction method".

Another method called "single-wavelength measurement method" was developed by Barbara and co-workers.[96,97] The main advantage of this method is that only one upconversion trace is needed for the calculation of solvation time. Therefore, this method is time-saving and relatively easier than the other one. The most important thing related to this method is the determination of optimal wavelength, which is good enough to represent the time scale of solvation dynamics for a particular fluorophore. For the determination of the optimal wavelength a quantity called spectral density at different wavelengths is plotted as a function of frequency corresponding to the emission maxima in various solvents. The optimal wavelength is that one where the spectral density is linearly dependent with the emission frequency. After determination of the optimal wavelength, fluorescence transient at that particular wavelength has to be collected to measure the solvation response. Barbara and co-workers have shown that the optimal wavelength for C480 is 420 nm, which is in the extreme blue end side of the emission spectrum of C480. On the contrary, Maroncelli et al.[68] have shown that in the case of Coumarin 153 (C153) single-wavelength measurement can be done at two wavelengths simultaneously. The two wavelengths are 476 nm (blue side of the fluorescence spectrum) and 556 nm (red side of the fluorescence spectrum). However, they have shown that between the two wavelengths the red one (556 nm) is the most optimal for C153. Shirota et al.[30] used this wavelength (560 nm) to study the solvation dynamics of C153 in a 1-propanol−water binary mixture using the single-wavelength measurement method. In our study, the main problem is that single-wavelength measurement cannot be performed at 420 nm as there is very low fluorescence intensity at this wavelength. In this situation, we have taken C153 as reference to choose an optimal wavelength for C480 (550 nm) which is in the red end side of the emission spectrum of C480. Additionally, in our previous study we have used this wavelength (550 nm) to study the solvation dynamics of C480 in DMSO−water binary mixtures and obtained very good results that are consistent with the spectral-reconstruction method.[61] In this method, upconversion traces of C480 at 550 nm in TBA−water and ethanol−water binary mixtures are analyzed by a triexponential function, eq 8, where the longest decay component is kept constant at the fluorescence lifetime of C480.

$$I_{550}(t) = a_{fl} \exp(-t/\tau_{fl}) + \sum_{i=1}^{2} a_{si} \exp(-t/\tau_{si}) \tag{8}$$

$$\sum_{i=1}^{2} a_{si} = 1 \tag{9}$$

where $I_{550}(t)$ is the time-dependent fluorescence intensity of C480 at 550 nm, a_{si} are the amplitudes of the solvation contribution, τ_{si} are the solvation time constants, and a_{fl} is the contribution of the fluorescence lifetime. The relative amplitudes of the two solvation components are normalized to be unity.

Average solvation times $(\langle\tau_s\rangle)$ are calculated using the following equation:

$$\langle\tau_s\rangle = \int_0^\infty C(t)\, \mathrm{d}t = \sum_{i=1}^{2} a_{si}\tau_{si} \tag{10}$$

We have also calculated other two characteristic times of solvation dynamics ($t_{1/e}$ and τ_0) for both binary systems.[30,66] The $t_{1/e}$ is the time required to attain the original amplitude $1/e$. τ_0 is calculated using the following equation:

$$\tau_0^{-1} = \sum_{i=1}^{2} a_{si}\tau_{si}^{-1} \tag{11}$$

Therefore, $\langle\tau_s\rangle$, $t_{1/e}$, and τ_0 are the long, intermediate, and short time characteristics of solvent reorganization dynamics, respectively. All information regarding single-wavelength measurements is tabulated in Tables S1 and S2 (Supporting Information).

Another important thing is that solvation dynamics generally deals with the time-resolved solvent response. However, spectral changes in time-resolved emission are a mixture of solvent response followed by the solute−solvent interaction. Ladanyi et al.[98] have shown how the solvation dynamics is affected by solute−solvent interaction in supercritical CO_2. Their study indicates that solute−solvent interaction has a significant contribution on the long time emission decay.

DOI: 10.1021/acs.jpcb.5b04931
J. Phys. Chem. B XXXX, XXX, XXX−XXX

Therefore, one can avoid the solute−solvent interaction in solvation dynamics only by measuring the solvation response through the single-wavelength measurement method. In this method solvation time is calculated from the growth components which arise solely from the solvent response. By considering all these points, in this work, single-wavelength measurements of C480 at 550 nm have been performed in TBA−water and ethanol−water binary mixtures.

Shirota et al.[30] nicely explained the advantages and disadvantages of the single-wavelength measurement method in comparison with the spectral-reconstruction procedure. In the upconversion technique, the main difficulty is to collect the emission decay too near to the excitation wavelength as discussed by Shirota et al. In our system, as the fluorescence spectrum is blue-shifted on going from neat water to neat alcohol, it is very difficult to collect the emission decays at the blue end side of the emission spectrum at high alcohol content. Due to this problem we cannot calculate the solvation time after $X_T/X_E = 0.6$ using the spectral-reconstruction method. On the other hand, in the case of the single-wavelength measurement method, after $X_T/X_E = 0.6$, fluorescence intensity of C480 at 550 nm becomes so much less that we are unable to collect the decay at that particular wavelength due to the same problem (blue-shifted fluorescence spectrum).

Maroncelli et al.[68] compared the two methods (spectral-reconstruction vs single-wavelength methods) for determining the solvation-response function. Their discussion led to the conclusions that (i) one should use the spectral-reconstruction method for accurate determination of the solvation-response function, (ii) the single-wavelength measurement method is perhaps used as a complementary method to check the results of spectral-reconstruction method, and (iii) the single-wavelength measurement method is appropriate for a series of related solvent systems, i.e., binary solvent mixture as a function of composition,[85] isotope substitution,[99] or at a series of different pressures or temperatures.[100] In these systems better precision is expected from the single-wavelength estimates compared to those of spectral reconstruction as the time required to collect the data in the former case is short with fixed instrumental parameters, and (iv) they have also pointed out that the ultimate accuracy of spectral reconstruction is higher compared to that of the single-wavelength method.

By considering all these discussions, we have first calculated solvation times of C480 in TBA−water and ethanol−water binary mixtures using the spectral-reconstruction method. After that, we have used the single-wavelength measurement method to verify our results. The results of the spectral-reconstruction method for both binary mixtures are summarized in Tables 1 and 2. C480 is extensively used as a solvation probe due to the dramatic increase in dipole moment upon photoexcitation ($\Delta\mu \approx 7$ D).[101]Additionally, due to its rigid structure, the other nonradiative pathway like intramolecular charge transfer (ICT) is inhibited compared to its other analogues.[102] Figure 5 represents the variation of solvation time of C480 in TBA−water (Figure 5a,b) and ethanol−water (Figure 5c−f) binary mixtures. For both binary mixtures we have detected two anomalous regions where solvation dynamics are significantly retarded with respect to the other regions of these binary mixtures. Interestingly, the results of two methods (spectral-reconstruction and single-wavelength methods) agree with one another, indicating rise in average solvation time in the ranges $X_T = 0.09-0.15$, $X_T = 0.40-0.46$ and $X_E = 0.06-0.08$, $X_E = 0.20-0.25$ for TBA−water and ethanol−water binary mixtures, respectively. Although, the prediction of the two methods is similar to identify the above stated regions, dissimilarities have been found in the case of average solvation time. Shirota et al.[30] stated that the primary disadvantage of the single-wavelength method is that the results do not agree perfectly with those from the spectral-reconstruction method. Therefore, the dissimilarities in solvation time are quite expected. Additionally, as our main aim is to detect the anomalous regions, the similarities in prediction for both the methods are the most important results in this study.

Actually, solvation dynamics in a binary mixture is completely different from that of neat water. In neat water, the major portion of solvation dynamics completes within 50 fs.[70] Therefore, it is expected that solvation response becomes faster with increasing water content in an aqueous binary mixture. However, on going from neat alcohol to neat water this trend is not maintained (some anomalous regions have been found). Previously, we have found a similar anomalous trend in solvation time (retardation of solvation dynamics at some particular regions) in DMSO−water binary mixtures due to some solvent clustering.[61] In this study, it is necessary to

Table 1. Decay Parameters of $C(t)$ of C480 in TBA−Water Binary Mixtures with Increasing TBA Content (Spectral-Reconstruction Method)

X_{TBA}	τ_{fast} (a_{fast}) (ps)	τ_{slow} (a_{slow}) (ps)	$\langle\tau_s\rangle$ (ps)[a]
0.02	1.53 (0.34)	5.12 (0.66)	3.90
0.03		2.98 (1.00)	2.98
0.04	0.70 (0.20)	3.87 (0.80)	3.24
0.05	1.02 (0.10)	5.27 (0.90)	4.84
0.06	2.26 (0.31)	12.03 (0.69)	9.00
0.07	3.45 (0.47)	17.50 (0.53)	10.90
0.09		18.84 (1.00)	18.84
0.15		14.70 (1.00)	14.70
0.21		13.77 (1.00)	13.77
0.29	4.28 (0.32)	14.72 (0.68)	11.38
0.40	4.90 (0.28)	16.05 (0.72)	12.93
0.46	2.08 (0.17)	18.50 (0.83)	15.71
0.54	1.24 (0.24)	9.07 (0.76)	7.19

[a]Error in experimental measurements ±10%.

Table 2. Decay Parameters of $C(t)$ of C480 in Ethanol−Water Binary Mixtures with Increasing Ethanol Content (Spectral-Reconstruction Method)

$X_{ethanol}$	τ_{fast} (a_{fast}) (ps)	τ_{slow} (a_{slow}) (ps)	$\langle\tau_s\rangle$ (ps)[a]
0.03	0.66 (0.31)	2.48 (0.69)	1.91
0.05	0.63 (0.26)	2.68 (0.74)	2.15
0.06	2.20 (0.51)	6.20 (0.49)	4.16
0.07	0.80 (0.32)	4.10 (0.68)	3.04
0.08	0.40 (0.10)	2.00 (0.90)	1.84
0.09	0.51 (0.38)	1.67 (0.62)	1.23
0.10	0.75 (0.29)	4.38 (0.71)	3.33
0.12	1.39 (0.13)	5.66 (0.87)	5.10
0.17	0.73 (0.04)	10.14 (0.96)	9.76
0.23		18.10 (1.00)	18.1
0.28		13.10 (1.00)	13.1
0.32	6.23 (0.21)	10.87 (0.79)	9.90
0.45	5.10 (0.29)	7.21 (0.71)	6.60
0.55	3.56 (0.41)	6.68 (0.59)	5.40

[a]Error in experimental measurements ±10%.

DOI: 10.1021/acs.jpcb.5b04931
J. Phys. Chem. B XXXX, XXX, XXX−XXX

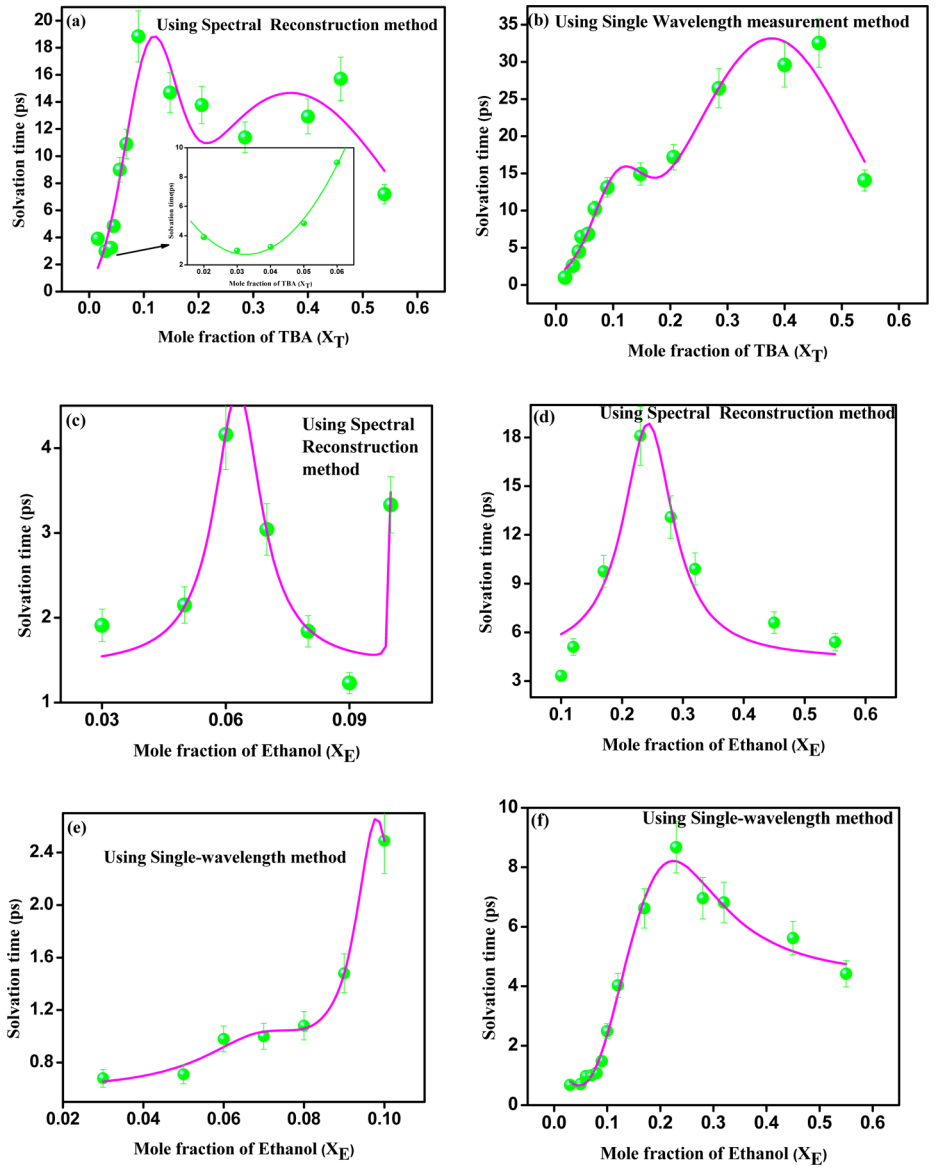

Figure 5. Variation of solvation time of C480 in TBA–water [(a) spectral-reconstruction method (inset shows the variation of solvation time in the range X_T = 0.02–0.06); (b) single-wavelength method] and ethanol–water [(c, d) spectral-reconstruction method; (e, f) single-wavelength method] binary mixtures.

focus the anomalous slowdown in solvation dynamics in terms of molecular level interpretations.

Very often, solvation dynamics (especially the long component of solvent correlation function) is discussed in terms of viscosity of the medium.[103,104] To check this effect, we have first measured the shear viscosity of two binary mixtures by varying TBA/ethanol content. The variation of shear viscosity of TBA–water and ethanol–water binary mixtures as a function of TBA/ethanol concentration is shown in Figures S3a and S3b (Supporting Information). We have seen that with increasing TBA/ethanol concentration viscosity of the medium increases. After reaching a maximum (5.32 cP for TBA–water and 2.55 cP for ethanol–water) at X_T = 0.43 and X_E = 0.23, viscosity of the medium decreases with further addition of TBA/ethanol. After that, we have plotted long decay components of solvent correlation function as a function of shear viscosity of the medium. These plots are shown in Figure S4a–c (Supporting Information). From Figure S4 we have observed that the long decay component of $C(t)$ reaches maxima in the ranges X_T = 0.09–0.15, X_T = 0.40–0.46 in TBA–water and X_E = 0.06–0.08, X_E = 0.20–0.25 in ethanol–water binary mixtures. Interestingly, the two regions with high alcohol content (X_T = 0.40–0.46 and X_E = 0.20–0.25) exactly match with the regions where the viscosity of the medium reaches maximum. Castner and co-workers have shown that the longer diffusive relaxation time constant (τ_2), which has been assigned to DMSO reorientation, is loosely correlated with the shear viscosity of the medium.[105] In correlation with their results, the anomalous slowdown in solvation response in the ranges X_T = 0.40–0.46 and X_E = 0.20–0.25 in TBA–water and ethanol–water binary mixtures is probably due to the higher shear viscosity of the medium. Note that, in our previous study we have also found a region, which arises from the higher shear viscosity of DMSO–water binary mixture.[61] It is very obvious that the shear viscosity of a binary mixture reaches a maximum at a certain composition due to some specific interactions between two mixing components.[13] Therefore, our observation is nicely correlated with the simulation work by Bagchi and co-

DOI: 10.1021/acs.jpcb.5b04931
J. Phys. Chem. B XXXX, XXX, XXX–XXX

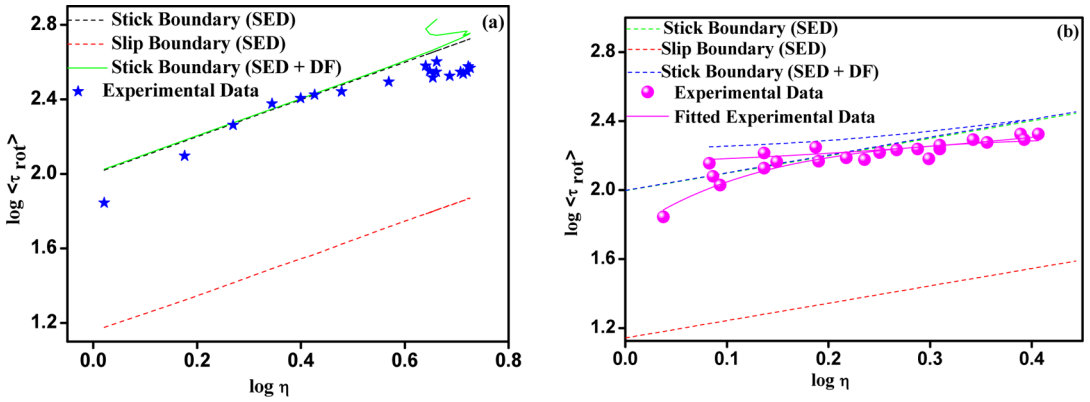

Figure 6. log–log plot of average rotational relaxation time ($\langle\tau_r\rangle$) of C480 in (a) TBA–water and (b) ethanol–water binary mixtures as a function of shear viscosity of the medium.

workers, who have observed reverse percolation transition of water molecules at higher TBA concentration ($X_T \sim 0.45$), where large spanning water clusters are converted into small clusters.[52] Biswas and co-workers have shown the structural transition in ethanol–water binary mixture at around $X_E \sim 0.20$ which corroborates our finding.[28] However, two other regions ($X_T = 0.09–0.15$ and $X_E = 0.06–0.08$) are not at all related to the shear viscosity of the medium.

Most of the thermodynamic properties exhibit deviation from ideal behavior at around 0.04 mole fraction of TBA in TBA–water binary mixtures. Note that experimental support in favor of this anomaly is not enough. Biswas and co-workers studied the charge transfer reaction of 4-(1-azetidinyl)-benzonitrile (P4C) in TBA–water binary mixtures.[31]They have shown that the long decay component (τ_{slow}) of P4C exhibits a minimum at TBA mole fraction ~0.04. In another work, the same group has calculated average activation energy for LE → CT conversion of P4C in TBA–water binary mixtures and plotted with respect to the mole fraction of TBA.[106] Interestingly, they have found a drastic change in the slope of that graph near around $X_T = 0.10$. However, they have not identified any minimum at around $X_T = 0.04$, although it was expected. They have mentioned that insufficient time resolution may be one of the reasons for this semiaccurate analysis. In our study, on going from $X_T = 0.02$ to 0.03 we have found a fall in average solvation time from 3.90 to 2.98 ps (Figure 4a and inset of Figure 5a). According to Bagchi et al., with the addition of TBA to water small TBA clusters are formed.[52] When the mole fraction of TBA approaches 0.05, small TBA clusters are agglomerated to large spanning cluster. The same agglomeration occurs when the temperature of the solution is increased.[107] This agglomeration of small TBA clusters drives the expelled water molecules toward the microscopic polar domains, hence increasing its polarity. Therefore, it is expected that this increased polarity (availability of free water molecules) may decrease the solvation time of C480. This is the probable reason for the faster solvation dynamics at $X_T = 0.03$.

It is very interesting to discuss about the regions which are viscosity independent ($X_T = 0.09–0.15$ and $X_E = 0.06–0.08$). Note that, in our previous study, we have detected slow solvation dynamics in the range $X_D = 0.12–0.17$ in DMSO–water binary mixtures due to formation of 1DMSO:2H_2O complex.[61] Through a series of work, Biswas and co-workers have shown the structural transition from the water like tetrahedral network to the zigzag alcohol like structure at around $X_T = 0.10$ in TBA–water binary mixtures.[28,31,106] Nishikawa et al.[107] pointed out that with increasing TBA concentration aggregation tendency increases and reaches a maximum in the range $X_T = 0.14–0.17$. The aggregation of TBA molecules at around $X_T = 0.10$ is further supported by Kusalik et al.[49] In the case of ethanol–water binary mixtures, Bagchi and co-workers have pointed out the percolation transition at very low mole fraction of ethanol ($X_T \sim 0.06–0.10$).[53] They concluded the percolation transition as a universal phenomenon at low solute concentration of aqueous amphiphilic binary mixtures. Our study indicates the slowdown in solvation response at around $X_T = 0.09–0.15$ and $X_E = 0.06–0.08$ in TBA–water and ethanol–water binary mixtures, respectively. In correlation with the previous literature reports, we think that structural transition may be the probable reason for this type of anomalous regions in TBA–water and ethanol–water binary mixtures.

In binary mixtures, one of the most interesting phenomena is the preferential solvation of solute molecules. Bagno et al.[108] studied the preferential solvation of phenol in DMSO–water binary mixture by ^{1}H nuclear Overhauser effect NMR spectroscopy. Their study indicates that phenol molecules are preferentially solvated by DMSO molecules at low DMSO content. In our study, from Tables 1 and 2 it is clear that the relative contribution of long decay component (assigned to continuous alcohol cluster) of solvent correlation function exhibits a sudden increase at around $X_T \sim 0.09$, 0.46 and $X_E \sim 0.20$ in TBA–water and ethanol–water binary mixtures, respectively. Therefore, particularly in these regions (where solvation time becomes highest) probe molecules are preferentially solvated by the large continuous alcohol cluster.

3.3. Rotational Dynamics of C480 in TBA–Water and Ethanol–Water Binary Mixtures. To corroborate our solvation dynamics results, we have performed time-resolved fluorescence anisotropy measurements of C480 in TBA–water and ethanol–water binary mixtures. Time-resolved fluorescence anisotropy provides information about the rotational dynamics of probe molecules. We have measured the anisotropy decays of C480 in TBA–water and ethanol–water binary mixtures by varying TBA/ethanol content. All the anisotropy decays were collected at emission maxima and nicely fitted by a single-exponential function as is evident from the values of fitting quality (χ^2) in Tables S3 and S4 in the Supporting Information. The rotational dynamics in common solvents were found to be single-exponential in nature and generally correlated with the

DOI: 10.1021/acs.jpcb.5b04931
J. Phys. Chem. B XXXX, XXX, XXX–XXX

Stokes−Einstein−Debye (SED) hydrodynamic theory as follows:[109]

$$\tau_r = \frac{\eta V}{kT} fC \tag{12}$$

In eq 12, the shape factor f compensates for any shape deviations (from its spherical geometry) of the solute dipole.[109] The solute−solvent interaction affects the rotational dynamics of the excited state dipole and is accounted by the solute−solvent coupling parameter (C). The value of C varies from zero, for the slip boundary condition, to 1 for the stick boundary condition. The shape factor (f) and the van der Waals volume (V) of C480 are assumed to be the same as those of C153 due to similar structure of both the coumarins, and the values are taken from previous literature.[101,110]Using the values of f, V, viscosity coefficient (η), and average rotational relaxation time ($\langle\tau_r\rangle$) in eq 12, we have calculated the values of C in TBA−water and ethanol−water binary mixtures. Rotational relaxation times of C480 along with the C values in both the binary mixtures are tabulated in Tables S3 and S4 in the Supporting Information.

Figure 6 shows the log−log plot of average rotational relaxation time ($\langle\tau_r\rangle$) of C480 as a function of shear viscosity in TBA−water (Figure 6a) and ethanol−water (Figure 6b) binary mixtures within the slip and stick boundary lines. The slip (or stick) boundary condition was obtained by connecting two τ_r values in the complete slip (or stick) condition of two neat solvents. The two τ_r values were calculated following the procedure described in ref 60. From Figure 6 and Tables S3 and S4 in the Supporting Information, we have observed the following points: (i) At very low mole fraction of TBA ($0.04 \leq X_T \leq 0.09$) or ethanol ($0.04 \leq X_E \leq 0.07$), the solute−solvent coupling parameter (C) follows the near stick or super-stick boundary region (i.e., above the stick boundary line). This observation indicates hindered rotational dynamics of probe molecules due to the prominent solute−solvent interaction. This also supports the results of anomalous solvation dynamics in the ranges $X_T = 0.09-0.15$ and $X_E = 0.06-0.08$ in TBA−water and ethanol−water binary mixtures, respectively.[60] (ii) We have observed a "hook-type" nature for both binary mixtures as found by Krishnamurthy et al. in HMPA−water binary mixtures.[88] (iii) SED boundary conditions (only by considering the viscous friction experienced by the probe molecule) are unable to explain the experimental results especially at high alcohol content.

Each and every binary mixture has its own characteristic shear viscosity and Debye dielectric relaxation time. Therefore, when a polar molecule rotates in a polar medium, it experiences friction due to hydrodynamics as well as dielectric friction. Hence, the total rotational relaxation time of a probe molecule is given by the following equation:

$$\tau_r(\text{total}) = \tau_r(\text{hydrodynamic}) + \tau_r(\text{dielectric friction}) \tag{13}$$

$$= \frac{\eta V}{kT} fC + \frac{4\pi\mu_{ex}^2}{3VkT} \frac{(\varepsilon - 1)}{(2\varepsilon + 1)^2} \tau_D \tag{14}$$

The first term in eq 14 is the contribution of hydrodynamic friction, and the second term is due to dielectric friction. In the second term, μ_e is the dipole moment of the solute in the excited state, ε the dielectric constant, τ_D the Debye dielectric relaxation time of the solvent, k Boltzmann's constant, and T the absolute temperature. The value of μ_e for C480 is taken from previous literature.[101] Values of ε and τ_D for TBA−water and ethanol−water binary mixtures are taken from refs 87 and 111, respectively.

Using eq 14, we have calculated the contributions of hydrodynamic as well as dielectric friction for every mole fraction of TBA−water and ethanol−water binary mixtures. Theoretically calculated rotational reorientation times of C480 (using SED theory and dielectric friction) in TBA−water and ethanol−water binary mixtures are tabulated in Tables S5 and S6 in the Supporting Information, respectively. By considering the contribution of dielectric friction along with the hydrodynamic friction, the combined boundary line nicely mimics the "hook-type" profile of the experimental data shown in Figure 6. Therefore, a detailed discussion is necessary about the applicability and limitations of hydrodynamic and dielectric friction with respect to the Figure 6.

From Figure 6, we have seen that at very low alcohol concentration ($X_T/X_E \leq 0.04$) SED theory alone can explain the experimental result very nicely. With increasing alcohol concentration ($0.04 \leq X_T \leq 0.09$ and $0.04 \leq X_E \leq 0.07$), experimentally observed rotational relaxation times of C480 follow the near stick or super-stick boundary line (this behavior is more pronounced in the case of TBA−water binary mixture). Dutt and co-workers observed a convex type profile in the case of nile blue, nile red, and resorufin in TBA−water binary mixture between 30% to 40% composition of TBA. According to them, the disagreement between experimental and theoretically predicted τ_r is due to the limitation of dielectric friction theory in its present form (the present form of dielectric friction is applicable for neat solvents).[87] On the other hand, Jena and co-workers explained the slow rotational relaxation of cresyl violet and fluorescein in alcohols in terms of specific solute−solvent interactions.[112]As the deviation is more pronounced in the case of TBA−water binary mixture, we think that there must be a specific interaction between C480 and solvent clusters which is more effective in the case of TBA−water. With further increase in alcohol concentration, we have observed a "hook-type" profile which is reproducible only by considering the contribution of dielectric friction along with the SED. Kenney−Wallace and co-workers also considered the contribution of dielectric friction to explain the rotational relaxation times of a few ionic probes in aqueous−propanol binary mixture.[113] In spite of some uncertainties about the applicability of dielectric friction theory in its present form and, also, the values of f and V for C480, the dielectric friction along with the hydrodynamic theory nicely explains the experimental results in our system.

3.4. Temperature Dependent Rotational Dynamics of C480 in TBA−Water and Ethanol−Water Binary Mixtures. Finney and co-workers (in 2007) have shown that the aggregation tendency of TBA molecules in TBA−water binary mixture increases with increase in temperature and reaches maximum at 80 °C.[58] In 2011, Biswas and co-workers have shown the temperature assisted aggregation of TBA molecules. However, they did not observe any aggregation maximum between 278 and 373 K.[106] In 2012, Gupta and Patey simulated TBA−water binary mixture using four different force fields. Surprisingly, among the four force fields two of them do not identify any aggregation of TBA molecules.[55] Therefore, the combined results of these three publications demand a further study to investigate the actual phenomena regarding the aggregation tendency of TBA molecules.

DOI: 10.1021/acs.jpcb.5b04931
J. Phys. Chem. B XXXX, XXX, XXX−XXX

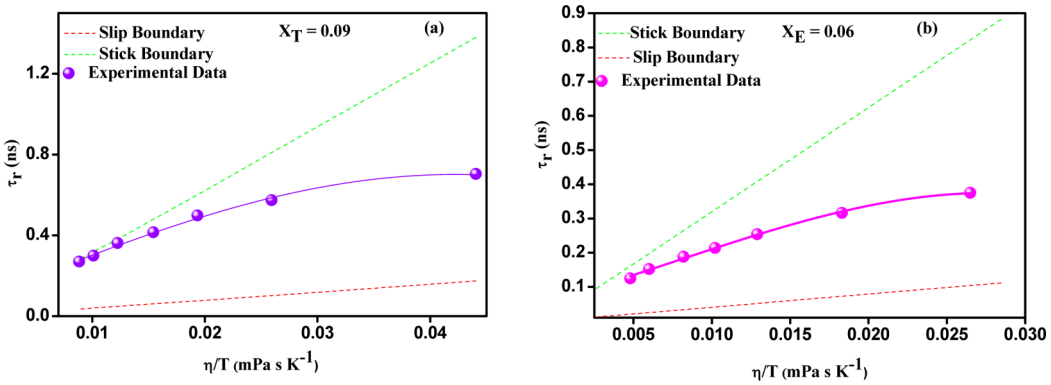

Figure 7. Plot of τ_r vs η/T for C480 in (a) TBA−water and (b) ethanol−water binary mixtures.

To investigate the effect of temperature on the aggregation behavior of TBA and ethanol molecules, we have performed temperature dependent anisotropy measurements of C480 in TBA−water and ethanol−water binary mixtures. From section 3.3, we have seen that, at very low mole fraction of TBA ($0.04 \leq X_T \leq 0.09$) and ethanol ($0.04 \leq X_E \leq 0.07$), the solute−solvent coupling parameter (C) follows the near stick or super-stick boundary region due to specific solute−solvent interaction. On the basis of this observation, we have chosen two mole fractions (for TBA−water; X_T = 0.09 and for ethanol−water; X_E = 0.06) to investigate the effect of temperature. We have collected anisotropy decays of C480 at X_T = 0.09 and X_E = 0.06 in TBA−water and ethanol−water binary mixtures by varying the temperature from 278 to 302 K at a regular interval of 4 °C. Temperature dependent anisotropy decays of C480 in both binary mixtures are shown in Figure S5a,b in the Supporting Information. All the anisotropy decays are nicely fitted by a single-exponential function, and the fitted parameters are tabulated in Table S7 in the Supporting Information. In order to calculate the reorientation time of C480 using SED hydrodynamic theory, we have taken the necessary information regarding the van der Waals volume of C480, axial radii (a, b, c) from ref 110. Now the diffusion coefficients D_i for the slip and stick boundary conditions were calculated from the friction coefficients (ζ_i) using the following equation:

$$D_i = \frac{kT}{\zeta_i} \tag{15}$$

The friction coefficients (ζ_i) with slip and stick boundary conditions were obtained from numerically tabulated values in the literature[114,115] assuming that the dimensionless friction coefficients vary linearly from the tabulated values. The reorientation times within the limit of slip and stick boundary conditions can now be calculated using the following equation:

$$\tau_r = \frac{1}{12}\left(\frac{4D_a + D_b + D_c}{D_aD_b + D_bD_c + D_cD_a}\right) \tag{16}$$

where D_a, D_b, and D_c are the diffusion coefficients along the a, b, and c axes, respectively. Figures 7a and 7b represent the plot of τ_r vs η/T for C480 within theoretically calculated slip and stick boundary lines. From Figure 7, we have seen that with increase in temperature τ_r follows the stick boundary line. We have calculated the solute−solvent interaction parameter (C) of C480 as a function of temperature (Table S7 in the Supporting Information). C varies from 0.54 to 1.15 in TBA−water (at X_T = 0.09) and 0.48 to 0.91 for ethanol−water (X_E = 0.06) binary mixtures on going from 278 to 302 K. Increase in the C value indicates increase in solute−solvent interaction. Therefore, it is clearly observed that, with increase in temperature, aggregation tendency of TBA/ethanol increases, and as a result hydrophobicity of the solution increases. C480 as a hydrophobic probe interacts more strongly with the hydrophobic solvent clusters with increase in temperature. Although we are unable to study the rotational behavior of C480 above 302 K due to the limited time resolution of our TCSPC setup, our present experimental results are sufficient to state that the aggregation tendency of TBA and ethanol molecule increases with increase in temperature.

4. CONCLUSION

In this work, we have investigated anomalous behavior of two alcohol−water (TBA−water and ethanol−water) binary mixtures by collecting ultrafast solvation response around a well-known solvation probe C480. The steady-state absorption and emission studies have given a preliminary indication about the anomalous nature of both binary mixtures. To confirm this, we have calculated average solvation time of C480 using two individual methods (spectral-reconstruction and single-wavelength methods). The results of the two methods (spectral-reconstruction and single-wavelength method) agree with one another, indicating the rise in average solvation time in the ranges X_T = 0.09−0.15, X_T = 0.40−0.46 and X_E = 0.06−0.08, X_E = 0.20−0.25 for TBA−water and ethanol−water binary mixtures, respectively. Predicted regions are consistent with the previous literature reports, mainly molecular dynamics simulation by Bagchi and co-workers[52,53] and steady-state, time-resolved studies by Biswas and co-workers.[28,106] Additionally, we have found a fall in average solvation time on going from X_T = 0.02 to 0.03. However, this type of behavior is totally absent in the case of ethanol−water binary mixture. Our results are consistent with the existence of an anomalous region at around X_T = 0.04. The rises in solvation time in the ranges X_T = 0.40−0.46 and X_E = 0.20−0.25 are probably due to the higher shear viscosity of the medium. In case of low alcohol content (X_T = 0.09−0.15 and X_E = 0.06−0.08), structural transition from water like tetrahedral network to zigzag alcohol like structure is the probable reason for slow solvation dynamics. We have also measured rotational reorientation times of C480 in these two binary mixtures. Hindered rotation of C480 in the ranges X_T = 0.04−0.09 and X_E = 0.03−0.07 in TBA−water and ethanol−water binary mixture corroborates our solvation dynamics results. To investigate the effect of temperature on

DOI: 10.1021/acs.jpcb.5b04931
J. Phys. Chem. B XXXX, XXX, XXX−XXX

the aggregation behavior of alcohol molecules, we have measured temperature dependent rotational dynamics of C480 in both binary mixtures. From this study, we have seen that with increase in temperature the solute−solvent coupling parameter (C) follows the stick boundary condition. This directly concludes temperature induced aggregation of alcohol molecules.

■ ASSOCIATED CONTENT

Supporting Information

Information on absorption maxima, emission maxima, Stokes shift, time-resolved emission spectra (TRES), shear viscosity, variation of solvation time (long decay component of solvent correlation function) of C480 as a function of shear viscosity of the medium, time-resolved anisotropy decays of C480 as a function of temperature, solvation parameters using single-wavelength measurement method at 550 nm of C480 in the entire region of TBA−water and ethanol−water binary mixtures, and rotational parameters of C480 in both binary mixtures. The Supporting Information is available free of charge on the ACS Publications website at DOI: 10.1021/acs.jpcb.5b04931.

■ AUTHOR INFORMATION

Corresponding Author

*E-mail: nilmoni@chem.iitkgp.ernet.in. Fax: 91-3222-255303.

Notes

The authors declare no competing financial interest.

■ ACKNOWLEDGMENTS

N.S. is thankful to SERB, Department of Science and Technology (DST), and Council of Scientific and Industrial Research (CSIR), Government of India, for generous research grants. D.B. and N.K. are thankful to IIT Kharagpur for research fellowship. A.R. is thankful to CSIR for research fellowship. We acknowledge the instrumental facility of National Centre for Ultrafast Processes (NCUFP), Chennai, India, for femtosecond fluorescence upconversion experiments. We are also thankful to Dr. C. Selvaraju, Dr. T. Senthil Kumar, and R. Suresh for their cooperation in recording femtosecond fluorescence lifetime decays.

■ REFERENCES

(1) Errington, J.; Debenedetti, P. Relationship between Structural Order and the Anomalies of Liquid Water. *Nature* **2001**, *409*, 318−321.

(2) Harris, K. R.; Woolf, L. A. Viscosity of Water + tert-Butyl Alcohol (2-Methyl-2-propanol) Mixtures at Low Temperatures and High Pressure. *J. Chem. Eng. Data* **2009**, *54*, 581−588.

(3) Kuchuk, V. I.; Shirokova, I. Y.; Golikova, E. V. Physicochemical Properties of Water−Alcohol Mixtures of a Homological Series of Lower Aliphatic Alcohols. *Glass Phys. Chem.* **2012**, *38*, 460−465.

(4) Srinivas, G.; Mukherjee, A.; Bagchi, B. Nonideality in the Composition Dependence of Viscosity in Binary Mixtures. *J. Chem. Phys.* **2001**, *114*, 6220−6228.

(5) Franks, F.; Ives, D. J. G. The structural Properties of Alcohol-Water Mixtures. *Q. Rev., Chem. Soc.* **1966**, *20*, 1−44.

(6) Westh, P. Thermal Expansivity, Molar Volume, and Heat Capacity of Liquid Dimethyl Sulfoxide-Water Mixtures at Subzero Temperatures. *J. Phys. Chem.* **1994**, *98*, 3222−3225.

(7) Zhang, L.; Wang, Q.; Liu, Y.-C.; Zhang, L.-Z. On the Mutual Diffusion Properties of Ethanol-Water Mixtures. *J. Chem. Phys.* **2006**, *125*, 104502(1)−104502(4).

(8) Kipkemboi, P. K.; Easteal, A. J. Self-Diffusion Coefficients of Each Component in Water + t-Butyl Alcohol and Water + t-Butylamine Binary Mixtures. *Bull. Chem. Soc. Jpn.* **1994**, *67*, 2956−2961.

(9) Pratt, K. C.; Wakeham, W. A. The Mutual Diffusion Coefficient for Binary Mixtures of Water and the Isomers of Propanol. *Proc. R. Soc. London, Ser. A* **1975**, *342*, 401−419.

(10) Lama, R. F.; Lu, B. C. Y. Excess Thermodynamic Properties of Aqueous Alcohol Solutions. *J. Chem. Eng. Data* **1965**, *10*, 216−219.

(11) Lai, J. W.; Lau, F.; Robb, D.; Westh, P.; Nielsen, G.; Trandum, C.; Hvidt, A.; Koga, Y. Excess Partial Molar Enthalpies, Entropies, Gibbs Energies, and Volumes in Aqueous Dimethylsulfoxide. *J. Solution Chem.* **1995**, *24*, 89−102.

(12) Markarian, S. A.; Terzyan, A. M. Surface Tension and Refractive Index of Dialkylsulfoxide + Water Mixtures at Several Temperatures. *J. Chem. Eng. Data* **2007**, *52*, 1704−1709.

(13) Catalán, J.; Díaz, C.; García-Blanco, F. Characterization of Binary Solvent Mixtures of DMSO with Water and Other Cosolvents. *J. Org. Chem.* **2001**, *66*, 5846−5852.

(14) Sakurai, M.; Nakamura, K.; Takenaka, N. Apparent Molar Volumes and Apparent Molar Adiabatic Compressions of Water in Some Alcohols. *Bull. Chem. Soc. Jpn.* **1994**, *67*, 352−359.

(15) Tamura, K.; Osaki, A.; Koga, Y. Compressibilities of Aqueous tert-Butanol in the Water-Rich Region at 25 °C: Partial molar Ñuctuations and Mixing Schemes. *Phys. Chem. Chem. Phys.* **1999**, *1*, 121−126.

(16) Egorov, G. I.; Makarov, D. M. The Compressibility of Water−Dimethyl Sulfoxide Mixtures Over the Temperature and Pressure Ranges 278−323.15 K and 1−1000 bar. *Russ. J. Phys. Chem. A* **2009**, *83*, 2058−2065.

(17) Kaatze, U.; Brai, M.; Scholle, F. D.; Pottel, R. Ultrasonic Absorption and Sound Velocity of Dimethyl Sulfoxide/Water mixtures in the Complete Composition Range. *J. Mol. Liq.* **1990**, *44*, 197−209.

(18) Brai, M.; Kaatze, U. Ultrasonic and Hypersonic Relaxations of Monohydric Aicohol/Water Mixtures. *J. Phys. Chem.* **1992**, *96*, 8946−8955.

(19) Rupprecht, A.; Kaatze, U. Model of Noncritical Concentration Fluctuations in Binary Liquids. Verification by Ultrasonic Spectrometry of Aqueous Systems and Evidence of Hydrophobic Effects. *J. Phys. Chem. A* **1999**, *103*, 6485−6491.

(20) Reis, J. C. R.; Douheret, G.; Davis, M. I.; Fjellanger, I. J.; Hoiland, H. Isentropic Expansion and Related Thermodynamic Properties of Non-Ionic Amphiphile−Water Mixtures. *Phys. Chem. Chem. Phys.* **2008**, *10*, 561−573.

(21) Banerjee, S.; Roy, S.; Bagchi, B. Enhanced Pair Hydrophobicity in the Water−Dimethylsulfoxide (DMSO) Binary Mixture at Low DMSO Concentrations. *J. Phys. Chem. B* **2010**, *114*, 12875−12882.

(22) Roy, S.; Banerjee, S.; Biyani, N.; Jana, B.; Bagchi, B. Theoretical and Computational Analysis of Static and Dynamic Anomalies in Water-DMSO Binary Mixture at Low DMSO Concentrations. *J. Phys. Chem. B* **2011**, *115*, 685−692.

(23) Roy, S.; Jana, B.; Bagchi, B. Dimethyl Sulfoxide Induced Structural Transformations and Non-Monotonic Concentration Dependence of Conformational Fluctuation around Active Site of Lysozyme. *J. Chem. Phys.* **2012**, *136*, 115103 (1)−115103 (10).

(24) Roy, S.; Bagchi, B. Solvation Dynamics of Tryptophan in Water-Dimethyl Sulfoxide Binary Mixture: In Search of Molecular Origin of Composition Dependent Multiple Anomalies. *J. Chem. Phys.* **2013**, *139*, 034308(1)−034308(10).

(25) Martins, L. R.; Tamashiro, A.; Laria, D.; Skaf, M. S. Solvation Dynamics of Coumarin 153 in Dimethylsulfoxide−Water Mixtures: Molecular Dynamics Simulations. *J. Chem. Phys.* **2003**, *118*, 5955−5963.

(26) Borin, I. A.; Skaf, M. S. Molecular Association Between Water and Dimethyl Sulfoxide in Solution: the Librational Dynamics of Water. *Chem. Phys. Lett.* **1998**, *296*, 125−130.

(27) Seth, D.; Sarkar, S.; Pramanik, R.; Ghatak, C.; Setua, P.; Sarkar, N. Photophysical Studies of a Hemicyanine Dye (LDS-698) in Dioxane-Water Mixture, in Different Alcohols, and in a Room Temperature Ionic Liquid. *J. Phys. Chem. B* **2009**, *113*, 6826−6833.

DOI: 10.1021/acs.jpcb.5b04931
J. Phys. Chem. B XXXX, XXX, XXX−XXX

(28) Pradhan, T.; Ghoshal, P.; Biswas, R. Structural Transition in Alcohol−Water Binary Mixtures: A Spectroscopic Study. *Proc. - Indian Acad. Sci., Chem. Sci.* **2008**, *120*, 275−287.
(29) Kashyap, H. K.; Biswas, R. Ions in a Binary Asymmetric Dipolar Mixture: Mole Fraction Dependent Born Energy of Solvation and Partial Solvent Polarization Structure. *J. Chem. Phys.* **2007**, *127*, 184502(1)−184502(15).
(30) Shirota, H.; Castner, E. W. Solvation in Highly Nonideal Solutions: A Study of Aqueous 1-Propanol Using the Coumarin 153 Probe. *J. Chem. Phys.* **2000**, *112*, 2367−2376.
(31) Pradhan, T.; Ghoshal, P.; Biswas, R. Excited State Intramolecular Charge Transfer Reaction in Binary Mixtures of Water and Tertiary Butanol (TBA): Alcohol Mole Fraction Dependence. *J. Phys. Chem. A* **2008**, *112*, 915−924.
(32) Zhang, X.; Zhu, Y.; Granick, S. Hydrophobicity at a Janus Interface. *Science* **2002**, *295*, 663−666.
(33) Glajch, J. L.; Kirkland, J. J.; Squire, K. M. Optimization of Solvent Strength and Selectivity for Reversed-Phase Liquid Chromatography Using an Inter-Active Mixture-Design Statistical Technique. *J. Chromatogr. A* **1980**, *199*, 57−79.
(34) Nguyen, N. H.; Rosen, B. M.; Jiang, X.; Fleischmann, S.; Percec, V. New Efficient Reaction Media for SET-LRP Produced from Binary Mixtures of Organic Solvents and H_2O. *J. Polym. Sci., Part A: Polym. Chem.* **2009**, *47*, 5577−5590.
(35) Frank, H. S.; Evans, M. W. Free Volume and Entropy in Condensed Systems III. Entropy in Binary Liquid Mixtures; Partial Molal Entropy in Dilute Solutions; Structure and Thermodynamics in Aqueous Electrolytes. *J. Chem. Phys.* **1945**, *13*, 507−532.
(36) Dixit, S.; Crain, J.; Poon, W. C. K.; Finney, J. L.; Soper, A. K. Molecular Segregation Observed in a Concentrated Alcohol−Water Solution. *Nature* **2002**, *416*, 829−832.
(37) Soper, A. K.; Finney, J. L. Hydration of Methanol in Aqueous Solution. *Phys. Rev. Lett.* **1993**, *71*, 4346−4349.
(38) Finney, J. L.; Bowron, D. T.; Daniel, R. M.; Timmins, P. A.; Roberts, M. A. Molecular and Mesoscale Structures in Hydrophobically Driven Aqueous Solutions. *Biophys. Chem.* **2003**, *105*, 391−409.
(39) Dougan, L.; Bates, S. P.; Hargreaves, R.; Fox, J. P.; Crain, J.; Finney, J. L.; Reat, V.; Soper, A. K. Methanol-Water Solutions: A Bi-Percolating Liquid Mixture. *J. Chem. Phys.* **2004**, *121*, 6456−6462.
(40) Murthy, S. S. N. Detailed Study of Ice Clathrate Relaxation: Evidence for the Existence of Clathrate Structures in Some Water-Alcohol Mixtures. *J. Phys. Chem. A* **1999**, *103*, 7927−7937.
(41) Euliss, G. W.; Sorensen, C. M. Dynamic Light Scattering Studies of Concentration Fluctuations in Aqueous t-Butyl Alcohol Solutions. *J. Chem. Phys.* **1984**, *80*, 4767−4773.
(42) Iwasaki, K.; Fujiyama, T. Light-Scattering Study of Clathrate Hydrate Formation in Binary Mixtures of tert-Butyl Alcohol and Water. 2. Temperature Effect. *J. Phys. Chem.* **1979**, *83*, 463−468.
(43) Subramanian, D.; Ivanov, D. A.; Yudin, I. K.; Anisimov, M. A.; Sengers, J. V. Mesoscale Inhomogeneities in Aqueous Solutions of 3-Methylpyridine and Tertiary Butyl Alcohol. *J. Chem. Eng. Data* **2011**, *56*, 1238−1248.
(44) Bowron, D. T.; Finney, J. L.; Soper, A. K. Structural Investigation of Solute-Solute Interactions in Aqueous Solutions of Tertiary Butanol. *J. Phys. Chem. B* **1998**, *102*, 3551−3563.
(45) Bowron, D. T.; Soper, A. K.; Finney, J. L. Temperature Dependence of the Structure of a 0.06 Mole Fraction Tertiary Butanol-Water Solution. *J. Chem. Phys.* **2001**, *114*, 6203−6219.
(46) D'Arrigo, G.; Teixeira, J. Small-Angle Neutron Scattering Study of D_2O−Alcohol Solutions. *J. Chem. Soc., Faraday Trans.* **1990**, *86*, 1503−1509.
(47) Borin, I. A.; Skaf, M. S. Molecular Association between Water and Dimethyl Sulfoxide in Solution: A Molecular Dynamics Simulation Study. *J. Chem. Phys.* **1999**, *110*, 6412−6420.
(48) Tanaka, H.; Nakanishi, K. Structure of Aqueous Solutions of Amphiphilies: t-Butyl Alcohol and Urea Solutions. *Fluid Phase Equilib.* **1993**, *83*, 77−84.
(49) Kusalik, P. G.; Lyubartsev, A. P.; Bergman, D. L.; Laaksonen, A. Computer Simulation Study of tert-Butyl Alcohol. 2. Structure in Aqueous Solution. *J. Phys. Chem. B* **2000**, *104*, 9533−9539.
(50) Lee, M. E.; van der Vegt, N. F. A. A New Force Field for Atomistic Simulations of Aqueous Tertiary Butanol Solutions. *J. Chem. Phys.* **2005**, *122*, 114509(1)−114509(13).
(51) Shulgin, I.; Ruckenstein, E. Kirkwood-Buff Integrals in Aqueous Alcohol Systems: Aggregation, Correlation Volume, and Local Composition. *J. Phys. Chem. B* **1999**, *103*, 872−877.
(52) Banerjee, S.; Furtado, J.; Bagchi, B. Fluctuating Micro-Heterogeneity in Water−tert-Butyl Alcohol Mixtures and Lambda-Type Divergence of the Mean Cluster Size with Phase Transition-Like Multiple Anomalies. *J. Chem. Phys.* **2014**, *140*, 194502(1)−194502(10).
(53) Banerjee, S.; Ghosh, R.; Bagchi, B. Structural Transformations, Composition Anomalies and a Dramatic Collapse of Linear Polymer Chains in Dilute Ethanol−Water Mixtures. *J. Phys. Chem. B* **2012**, *116*, 3713−3722.
(54) Banerjee, S.; Bagchi, B. Stability of Fluctuating and Transient Aggregates of Amphiphilic Solutes in Aqueous Binary Mixtures: Studies of Dimethyl Sulfoxide, Ethanol, and tert-Butyl Alcohol. *J. Chem. Phys.* **2013**, *139*, 164301(1)−164301(7).
(55) Gupta, R.; Patey, G. N. Aggregation in Dilute Aqueous tert-Butyl Alcohol Solutions: Insights from Large-Scale Simulations. *J. Chem. Phys.* **2012**, *137*, 034509(1)−034509(12).
(56) Ben-Amotz, D. Hydrophobic Ambivalence: Teetering on the Edge of Randomness. *J. Phys. Chem. Lett.* **2015**, *6*, 1696−1701.
(57) Rankin, B. M.; Ben-Amotz, D.; van der Post, S. T.; Bakker, H. J. Contacts between Alcohols in Water Are Random Rather Than Hydrophobic. *J. Phys. Chem. Lett.* **2015**, *6*, 688−692.
(58) Bowron, D. T.; Finney, J. L. Association and Dissociation of an Aqueous Amphiphile at Elevated Temperatures. *J. Phys. Chem. B* **2007**, *111*, 9838−9852.
(59) Subramanian, D.; Boughter, C. T.; Klauda, J. B.; Hammouda, B.; Anisimov, M. A. Mesoscale Inhomogeneities in Aqueous Solutions of Small Amphiphilic Molecules. *Faraday Discuss.* **2013**, *167*, 217−238.
(60) Koley, S.; Kaur, H.; Ghosh, S. Probe Dependent Anomalies in the Solvation Dynamics of Coumarin Dyes in Dimethyl Sulfoxide−Glycerol Binary Solvent: Confirming the Local Environments are Different for Coumarin Dyes. *Phys. Chem. Chem. Phys.* **2014**, *16*, 22352−22363.
(61) Banik, D.; Kundu, N.; Kuchlyan, J.; Roy, A.; Banerjee, C.; Ghosh, S.; Sarkar, N. Picosecond Solvation Dynamics - a Potential Viewer of DMSO - Water Binary Mixtures. *J. Chem. Phys.* **2015**, *142*, 054505 (1)−054505 (10).
(62) Gardecki, J.; Horng, M. L.; Papazyan, A.; Maroncelli, M. Ultrafast Measurements of the Dynamics of Solvation in Polar and Non-Dipolar Solvents. *J. Mol. Liq.* **1995**, *65/66*, 49−57.
(63) Rosenthal, S. J.; Jimenez, R.; Fleming, G. R.; Kumar, P. V.; Maroncelli, M. Solvation Dynamics in Methanol: Experimental and Molecular Dynamics Simulation Studies. *J. Mol. Liq.* **1994**, *60*, 25−56.
(64) Maroncelli, M. The Dynamics of Solvation in Polar Liquids. *J. Mol. Liq.* **1993**, *57*, 1−37.
(65) Castner, E. W., Jr.; Maroncelli, M.; Fleming, G. R. Subpicosecond Resolution Studies of Solvation Dynamics in Polar Aprotic and Alcohol Solvents. *J. Chem. Phys.* **1987**, *86*, 1090−1097.
(66) Horng, M. L.; Gardecki, J. A.; Papazyan, A.; Maroncelli, M. Subpicosecond Measurements of Polar Solvation Dynamics: Coumarin 153 Revisited. *J. Phys. Chem.* **1995**, *99*, 17311−17337.
(67) Maroncelli, M.; Fleming, G. R. Picosecond Solvation Dynamics of Coumarin 153: The Importance of Molecular Aspects of Solvation. *J. Chem. Phys.* **1987**, *86*, 6221−6239.
(68) Gardecki, J. A.; Maroncelli, M. Comparison of the Single-Wavelength and Spectral-Reconstruction Methods for Determining the Solvation-Response Function. *J. Phys. Chem. A* **1999**, *103*, 1187−1197.
(69) Gardecki, J. A.; Maroncelli, M. Solvation and Rotational Dynamics in Acetonitrile/Propylene Carbonate Mixtures: a Binary

DOI: 10.1021/acs.jpcb.5b04931
J. Phys. Chem. B XXXX, XXX, XXX−XXX

System for Use in Dynamical Solvent Effect Studies. *Chem. Phys. Lett.* **1999**, *301*, 571−578.
(70) Jimenez, R.; Fleming, G. R.; Kumar, P. V.; Maroncelli, M. Femtosecond Solvation Dynamics of Water. *Nature* **1994**, *369*, 471−473.
(71) Jarzeba, W.; Walker, G. C.; Johnson, A. E.; Kahlow, M. A.; Barbara, P. F. Femtosecond Microscopic Solvation Dynamics of Aqueous Solutions. *J. Phys. Chem.* **1988**, *92*, 7039−7041.
(72) Barbara, P. F.; Jarzeba, W. Ultrafast Photochemical Intramolecular Charge and Excited State Solvation. *Adv. Photochem.* **1990**, *15*, 1−68.
(73) Sarkar, N.; Datta, A.; Das, S.; Bhattacharyya, K. Solvation Dynamics of Coumarin 480 in Micelles. *J. Phys. Chem.* **1996**, *100*, 15483−15486.
(74) Sarkar, N.; Das, K.; Datta, A.; Das, S.; Bhattacharyya, K. Solvation Dynamics of Coumarin 480 in Reverse Micelles. Slow Relaxation of Water Molecules. *J. Phys. Chem.* **1996**, *100*, 10523−10527.
(75) Datta, A.; Pal, S. K.; Mandal, D.; Bhattacharyya, K. Solvation Dynamics of Coumarin 480 in Vesicles. *J. Phys. Chem. B* **1998**, *102*, 6114−6117.
(76) Bhattacharyya, K. Solvation Dynamics and Proton Transfer in Supramolecular Assemblies. *Acc. Chem. Res.* **2003**, *36*, 95−101.
(77) Bagchi, B. Water Dynamics in the Hydration Layer Around Proteins and Micelles. *Chem. Rev.* **2005**, *105*, 3197−3219.
(78) Nandi, N.; Bhattacharyya, K.; Bagchi, B. Dielectric Relaxation and Solvation Dynamics of Water in Complex Chemical and Biological Systems. *Chem. Rev.* **2000**, *100*, 2013−2045.
(79) Willard, D. M.; Riter, R. E.; Levinger, N. E. Dynamics of Polar Solvation in Lecithin/Water/Cyclohexane Reverse Micelles. *J. Am. Chem. Soc.* **1998**, *120*, 4151−4160.
(80) Riter, R. E.; Undiks, E. P.; Levinger, N. E. Impact of Counterion on Water Motion in Aerosol OT Reverse Micelles. *J. Am. Chem. Soc.* **1998**, *120*, 6062−6067.
(81) Shirota, H.; Tamoto, Y.; Segawa, H. Dynamic Fluorescence Probing of the Microenvironment of Sodium Dodecyl Sulfate Micelle Solutions: Surfactant Concentration Dependence and Solvent Isotope Effect. *J. Phys. Chem. A* **2004**, *108*, 3244−3252.
(82) Tamoto, Y.; Segawa, H.; Shirota, H. Solvation Dynamics in Aqueous Anionic and Cationic Micelle Solutions: Sodium Alkyl Sulfate and Alkyltrimethylammonium Bromide. *Langmuir* **2005**, *21*, 3757−3764.
(83) Frauchiger, L.; Shirota, H.; Uhrich, K. E.; Castner, E. W., Jr. Dynamic Fluorescence Probing of the Local Environments within Amphiphilic Starlike Macromolecules. *J. Phys. Chem. B* **2002**, *106*, 7463−7468.
(84) Kahlow, M. A.; Jarzeba, W.; Kang, T. J.; Barbara, P. F. Femtosecond Resolved Solvation Dynamics in Polar Solvents. *J. Chem. Phys.* **1989**, *90*, 151−158.
(85) Jarzeba, W.; Walker, G. C.; Johnson, A. E.; Barbara, P. F. Nonexponential Solvation Dynamics of Simple Liquids and Mixtures. *Chem. Phys.* **1991**, *152*, 57−68.
(86) Cichos, F.; Willert, A.; Rempel, U.; von Borczyskowski, C. V. Solvation Dynamics in Mixtures of Polar and Nonpolar Solvents. *J. Phys. Chem. A* **1997**, *101*, 8179−8185.
(87) Dutt, G. B.; Doraiswamy, S.; Periasamy, N. Molecular Reorientation Dynamics of Polar Dye Probes in Tertiary-Butyl Alcohol-Water Mixtures. *J. Chem. Phys.* **1991**, *94*, 5360−5368.
(88) Krishnamurthy, M.; Khan, K. K.; Doraiswamy, S. Rotational Diffusion Kinetics of Polar Solutes in Hexamethylphosphoramide-Water Systems. *J. Chem. Phys.* **1993**, *98*, 8640−8646.
(89) Mandal, S.; Ghosh, S.; Banerjee, C.; Kuchlyan, J.; Sarkar, N. Roles of Viscosity, Polarity, and Hydrogen-Bonding Ability of a Pyrrolidinium Ionic Liquid and Its Binary Mixtures in the Photophysics and Rotational Dynamics of the Potent Excited-State Intramolecular Proton-Transfer Probe 2,2′-Bipyridine-3,3′-diol. *J. Phys. Chem. B* **2013**, *117*, 6789−6800.
(90) Das, S. K.; Sarkar, M. Rotational Dynamics of Coumarin-153 and 4-Aminophthalimide in 1-Ethyl-3-methylimidazolium Alkylsulfate Ionic Liquids: Effect of Alkyl Chain Length on the Rotational Dynamics. *J. Phys. Chem. B* **2012**, *116*, 194−202.
(91) Das, S. K.; Sahu, P. K.; Sarkar, M. Diffusion−Viscosity Decoupling in Solute Rotation and Solvent Relaxation of Coumarin153 in Ionic Liquids Containing Fluoroalkylphosphate (FAP) Anion: A Thermophysical and Photophysical Study. *J. Phys. Chem. B* **2013**, *117*, 636−647.
(92) Furniss, B. S.; Hannaford, A. J.; Smith, P. W. G.; Tatchell, A. R. *Vogel's Textbook of Practical Organic Chemistry*, 5th ed.; John Wiley & Sons, Inc.: New York, 1989.
(93) Hazra, P.; Chakrabarty, D.; Sarkar, N. Solvation Dynamics of Coumarin 153 in Aqueous and Non-aqueous Reverse Micelles. *Chem. Phys. Lett.* **2003**, *371*, 553−562.
(94) Dhenadhayalan, N.; Selvaraju, C. Role of Photoionization on the Dynamics and Mechanism of Photoinduced Electron Transfer Reaction of Coumarin 307 in Micelles. *J. Phys. Chem. B* **2012**, *116*, 4908−4920.
(95) Laage, D.; Thompson, W. H.; Blanchard-Desce, M.; Hynes, J. T. Charged Push-Pull Polyenes in Solution: Anomalous Solvatochromism and Nonlinear Optical Properties. *J. Phys. Chem. A* **2003**, *107*, 6032−6046.
(96) Nagarajan, V.; Brearley, A. M.; Kang, T. J.; Barbara, P. F. Time-Resolved Spectroscopic Measurements on Microscopic Solvation Dynamics. *J. Chem. Phys.* **1987**, *86*, 3183−3196.
(97) Kahlow, M. A.; Kang, T. J.; Barbara, P. F. Transient Solvation of Polar Dye Molecules in Polar Aprotic Solvents. *J. Chem. Phys.* **1988**, *88*, 2372−2378.
(98) Ladanyi, B. M.; Nugent, S. The Effects of Solute-Solvent Electrostatic Interactions on Solvation Dynamics in Supercritical CO_2. *J. Chem. Phys.* **2006**, *124*, 044505(1)−044505(11).
(99) Shirota, H.; Pal, H.; Tominaga, K.; Yoshihara, K. Deuterium Isotope Effect on the Solvation Dynamics of Methanol: CH_3OH, CH_3OD, CD_3OH, and CD_3OD. *J. Phys. Chem.* **1996**, *100*, 14575−14577.
(100) Nagasawa, Y.; Yartsev, A. P.; Tominaga, K.; Johnson, A. E.; Yoshihara, K. Temperature Dependence of Ultrafast Intermolecular Electron Transfer Faster than Solvation Process. *J. Chem. Phys.* **1994**, *101*, 5717−5726.
(101) Gupta, S.; Rafiq, S.; Kundu, M.; Sen, P. Origin of Strong Synergism in Weakly Perturbed Binary Solvent System: A Case Study of Primary Alcohols and Chlorinated Methanes. *J. Phys. Chem. B* **2012**, *116*, 1345−1355.
(102) Nag, A.; Chakrabarty, T.; Bhattacharyya, K. Effect of Gamma.-Cyclodextrin on the Intramolecular Charge Transfer Processes in Aminocoumarin Laser Dyes. *J. Phys. Chem.* **1990**, *94*, 4203−4206.
(103) Samanta, A. Solvation Dynamics in Ionic Liquids: What We Have Learned from the Dynamic Fluorescence Stokes Shift Studies. *J. Phys. Chem. Lett.* **2010**, *1*, 1557−1562.
(104) Chakrabarty, D.; Hazra, P.; Chakraborty, A.; Seth, D.; Sarkar, N. Dynamics of Solvent Relaxation in Room Temperature Ionic Liquids. *Chem. Phys. Lett.* **2003**, *381*, 697−704.
(105) Wiewiór, P. P.; Shirota, H.; Castner, E. W., Jr. Aqueous Dimethyl Sulfoxide Solutions: Inter- and Intra-Molecular Dynamics. *J. Chem. Phys.* **2002**, *116*, 4643−4654.
(106) Gazi, H. A. R.; Biswas, R. Heterogeneity in Binary Mixtures of (Water + Tertiary Butanol): Temperature Dependence across Mixture Composition. *J. Phys. Chem. A* **2011**, *115*, 2447−2455.
(107) Nishikawa, K.; Hayashi, H.; Iijima, T. Temperature Dependence of the Concentration Fluctuation, the Kirkwood-Buff Parameters, and the Correlation Length of fed-Butyl Alcohol and Water Mixtures Studied by Small-Angle X-ray Scattering. *J. Phys. Chem.* **1989**, *93*, 6559−6565.
(108) Bagno, A.; Campulla, M.; Pirana, M.; Scorrano, G.; Stiz, S. Preferential Solvation of Organic Species in Binary Solvent Mixtures Probed by Intermolecular 1H NOESY NMR Spectroscopy. *Chem. - Eur. J.* **1999**, *5*, 1291−1300.
(109) Perrin, F. Mouvement Brownien d'un Ellipsoide - I. Dispersion Diélectrique Pour Des Molecules Ellipsoidales. *J. Phys. Radium* **1934**, *5*, 497−511.

DOI: 10.1021/acs.jpcb.5b04931
J. Phys. Chem. B XXXX, XXX, XXX−XXX

(110) Dutt, G. B.; Ghanty, T. K. Rotational Diffusion of Coumarins in Electrolyte Solutions: The Role of Ion Pairs. *J. Phys. Chem. B* **2003**, *107*, 3257−3264.
(111) Dutt, G. B.; Doraiswamy, S. Picosecond Reorientational Dynamics of Polar Dye Probes in Binary Aqueous Mixtures. *J. Chem. Phys.* **1992**, *96*, 2475−2491.
(112) Von Jena, A.; Lessing, H. E. Rotational Diffusion of Dyes in Solvents of Low Viscosity from Transient-Dichroism Experiments. *Chem. Phys. Lett.* **1981**, *78*, 187−193.
(113) Templeton, E. F. G.; Kenney-Wallace, G. A. Correlation between Molecular Reorientation Dynamics of Ionic Probes in Pdlar Fluids and Dielectric Friction by Picosecond Modulation Spectroscopy. *J. Phys. Chem.* **1986**, *90*, 5441−5448.
(114) Sension, R. J.; Hochstrasser, R. M. Comment on: Rotational Friction Coefficients for Ellipsoids and Chemical Molecules with Slip Boundary Conditions. *J. Chem. Phys.* **1993**, *98*, 2490.
(115) Small, E. W.; Isenberg, I. Hydrodynamic Properties of a Rigid Molecule: Rotational and Linear Diffusion and Fluorescence Anisotropy. *Biopolymers* **1977**, *16*, 1907−1928.

DOI: 10.1021/acs.jpcb.5b04931
J. Phys. Chem. B XXXX, XXX, XXX−XXX